URSI AP-RASC, Sydney, Australia, 17 – 22 August 2025

Analytical Estimates of the Fundamental-Mode Fields in Regular Polygonal Waveguides with Application to Tri-Ridged Orthomode Transducers

Aidan Lötter(1) and Dirk I.L. de Villiers(1)
(1) Department of Electrical and Electronic Engineering, Stellenbosch University, Stellenbosch, 7600, South Africa

Abstract

This paper presents an analytical approach to estimate the fundamental transverse electric and transverse magnetic field distributions in regular polygonal waveguides as a finite sum of cylindrical waves. This approximation uses previously published empirical formulas to estimate the wavenumber of the fundamental modes of interest. It is shown that the fields can be approximated to within a few percent accuracy, as compared to the numerical solutions, by only including two cylindrical modes. The derived field expressions are further applied to the analysis of a tri-ridged orthomode transducer, demonstrating a quantitative relationship between the return loss parameters.

1 Introduction

Radio telescope reflector antennas, such as the Square Kilometre Array (SKA)[1] and the next generation Very Large Array (ngVLA) [2], highlight the need for highly sensitive receivers capable of operating over wide frequency ranges, often exceeding an octave. The quad-ridged flared horn (QRFH) antenna is currently one of the most promising technologies and has been shown to operate in more than 3:1 bandwidths [3, 4, 5]. The QRFH can excite a problematic trapped mode when the ridges are not perfectly excited with the differential TE_{11} odd mode [6]. Work done in [7, 8, 9] has shown that three-fold symmetry can be used to create a three-port OMT with a large single-mode bandwidth. In [8], a theoretical tri-ridged OMT prototype is developed and analysis is performed to calculate the return loss of the left-hand circularly polarized (LHCP)(S_{LL}) wave in the OMT (without loss of generality with respect to other polarizations). However, when integrating the OMT with a TRFH antenna, knowing the return loss of the fundamental waveguide mode (S_{MM}) is useful, since this is the excitation field used when simulating the antenna (the final radiation pattern is synthesized by rotation and superposition of the resulting single mode pattern). Although the relationship between S_{MM} and S_{LL} may seem intuitive, that is, a small $|S_{LL}|$ implies a small $|S_{MM}|$, finding a quantitative relation is important for optimization and design work.

In this paper, a method is developed to solve the fundamental mode field distribution in general regular polygonal waveguides (RPWs). Instead of using an eigenvalue approach to estimate the cutoff wavenumber, the empirical equations presented in [10, 11] are used. Using this result, an explicit formula for the field distribution of the fundamental TE or TM modes can be derived from a truncated sum of analytical cylindrical modes. The resulting estimated field distribution of a triangular waveguide is used, along with further analysis of the tri-ridged OMT, to prove the hypothesized relationships between the return loss values that $S_{MM} = S_{LL}$. Section 2 presents the theoretical development, followed by the results in Section 3, and the application thereof to the tri-ridged OMT in Section 4.

2 Theory

2.1 General Cylindrical Modes

Consider the homogeneous Helmholtz equation for a transversal wave function Φ (representing electric or magnetic fields)

$$\nabla_{\mathrm{t}}^2\Phi + k_{\mathrm{c}}\Phi = 0, \tag{1}$$

where k_{c} indicates the wavenumber and ∇_t explicitly restricts the spacial derivative to the plane transverse to the direction of propagation. The standard transverse- electric (TE) and magnetic (TM) boundary conditions apply as

$$\text{TM:} \quad \Phi = 0; \quad \text{TE:} \quad \frac{\partial \Phi}{\partial \nu} = 0, \tag{2}$$

where ν is the normal vector on the waveguide walls in the transversal plane. The solutions to (1) in the cylindrical coordinate system, with ϕ the azimuth angle measured from the x-axis and ρ the distance from the z-axis, are very well known and, for the longitudinal z-component of the total field, take the form

$$\Phi_z(\rho,\phi) = \sum_{n=0}^{\infty} J_n(k_{\mathrm{c}}\rho)(A_n \sin(n\phi) + B_n \cos(n\phi)), \tag{3}$$

where J_n is the Bessel function of the first kind, A_n and B_n are integration constants and n is an integer. All other field components can easily be calculated as spacial derivatives of the appropriate z-component as described in, for instance, [12].

2.2 Application to RPWs

Now, consider the (arbitrarily) x-polarised TE fields in an RPW with s sides, numbered by the natural number $k < s$,

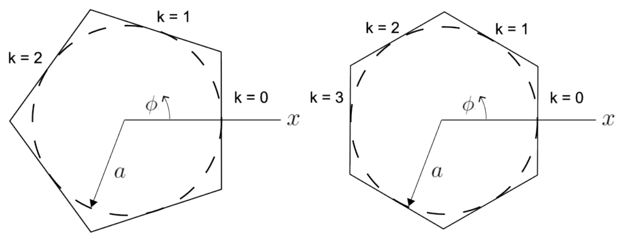

(a) Pentagon **(b)** Hexagon

Figure 1. Pentagon and hexagon defined with an inscribed circle of radius a.

shown in Fig. 1. In this case $\Phi_z(\rho, \phi)$ represents the magnetic field, and the Neumann boundary condition in (2), with $\nu = \rho$, implies at least vanishing ϕ-components of the electric field where the inscribed circle of Fig. 1 is tangential to the waveguide walls at

$$\phi_0 = \frac{2\pi k}{s};\ k = 0, 1, \ldots, s-1;\ \rho = a. \tag{4}$$

Explicitly, the boundary condition becomes

$$\sum_{n=0}^{\infty} A_n J_n'(k_c\rho)\sin(n\phi) + B_n J_n'(k_c\rho)\cos(n\phi) = 0, \tag{5}$$

with J' indicating the derivative of J with respect to its argument. The polarization orientation sets $B_n = 0$, and $n \neq 0$ to avoid the trivial null-field solution. The simplest analytical field solution which satisfies the boundary conditions require only two cylindrical modes to be retained, with the first having $n = 1$. Then, from (5),

$$\frac{A_1 J_1'(k_c a)}{A_n J_n'(k_c a)} = -\frac{\sin(n\frac{2\pi k}{s})}{\sin(\frac{2\pi k}{s})}, \tag{6}$$

where the left hand side is a constant ratio (independent of k). The right hand side will be constant when adding integer factors of 2π to the argument in the denominator, implying

$$\frac{n2\pi k}{s} = \pm m2\pi k + \frac{2\pi k}{s}, \tag{7}$$

with m an integer not equal to 0, allowing n to be solved as

$$n = |\pm sm + 1|. \tag{8}$$

The absolute value is due to the symmetry of negative integer order Bessel functions. Therefore, considering only positive n, the lowest order cylindrical mode, corresponding to the fundamental mode for a given s, is $n = s-1$. To solve Φ_z from (6), the exact value of k_c can be calculated for triangular and square waveguides using the expressions in [13] and [12] respectively, and analytically approximated for polygons with five sides and more by using those in [11]. Everything is thus in place to solve for A_{s-1} when normalising $A_1 = 1$ from (6), which can be substituted back into (5) to get a simple (two-mode) estimate of the fundamental mode field distribution in any RPW.

Next, consider the TM field for an RPW, oriented such that $A_n = 0$ (without loss of generality). Now $\Phi_z(\rho, \phi)$ represents the electric field and the Dirichlet boundary condition in (2) forces the z-component of the electric field to vanish at least at the points in (4). The first cylindrical mode has $n = 0$, which gives the two-mode estimate directly from (3) as

$$\frac{A_0 J_0(k_c a)}{A_n J_n(k_c a)} = -\frac{\cos(n\frac{2\pi k}{s})}{1}, \tag{9}$$

for $n \neq 0$. The simplest solution is found by setting the argument of the numerator of the right-hand-side to 0, which yields

$$n = |\pm sm|, \tag{10}$$

and is general to within a scaling factor of the integration constants. The lowest order cylindrical mode, corresponding to the fundamental TM mode for a given s, is therefore the one with $n = s$. To solve for Φ_z, k_c is calculated as for the TE modes.

3 Results

For verification, the fundamental mode field distributions for RPWs with 3 to 10 sides were calculated numerically in CST Microwave Studio [14]. For concise comparison, the axial fields for the TE and TM modes were exported from CST with a phase of 90° and 0°, respectively, so the instantaneous fields would be purely imaginary and purely real for the TE and TM modes. The axial fields of these modes are compared to the analytical estimation with two cylindrical modes included. Simulated and estimated field plots for a triangle, pentagon, and hexagon are shown for the TE and TM modes in Figs. 2a and 2b respectively. Simulated and estimated fields were normalised by their respective maximums (occurring in the corners and in the centre for the TE and TM modes respectively) to calculate the error plot. For error calculations, the absolute value of the difference was taken and multiplied by 100% as

$$\text{Error\%} = 100 \times \left| \frac{\Phi_{\text{sim}}}{\max(|\Phi_{\text{sim}}|)} - \frac{\Phi_{\text{appr}}}{\max(|\Phi_{\text{appr}}|)} \right|, \tag{11}$$

where the subscripts 'sim' and 'appr' refer to simulated and approximated fields respectively. The colour of the error plot is scaled with the maximum error for each shape. Table 1 shows the root-mean-square (RMS) error for each estimation for up to 10 sides. Investigating Figs. 2a and 2b, the largest errors typically appear to occur in the corners of the RPW, with the error generally decreasing towards the centre.

4 Application to the Tri-Ridged OMT

A tri-ridged waveguide is shown in Fig. 3. Each ridge within the waveguide is 120° apart and has an excitation

Table 1. RMS percentage error for TE and TM mode estimation

	3	**4**	**5**	**6**	**7**	**8**	**9**	**10**
TE	1.35	0.51	1.08	0.71	0.59	0.34	0.34	0.71
TM	2.27	0.25	1.94	1.4	1.09	0.85	0.73	0.86

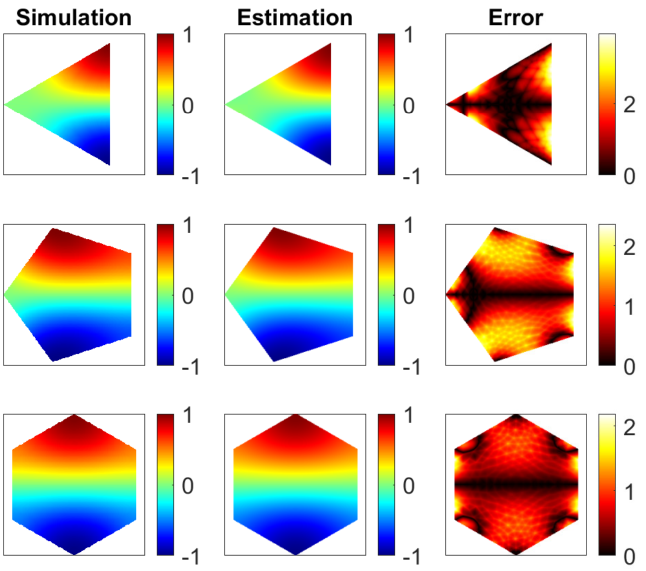

(a) TE modes

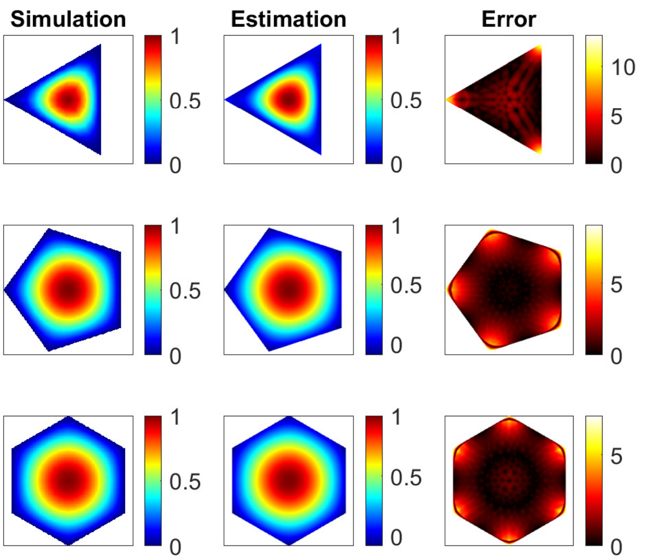

(b) TM modes

Figure 2. Simulated and approximated axial field plots for the normalised fundamental TE (top) and TM (bottom) modes for triangular, pentagonal and hexagonal waveguides. Approximated fields, shown in the middle column, contain two cylindrical modes. The error plots, shown in the right-hand column, are generated using (11).

port associated with it. Port 1 lies in the magnetic symmetry plane, with ports 2 and 3 symmetrically about it. The magnetic symmetry plane enforces the orientation of fundamental mode to match with the example in the RPW. A central TEM port is included in the tri-ridge design in [8, 9], however, the TEM mode does not couple into the fundamental mode and therefore the analysis with and without the central port would yield the same result. In [8], the re-

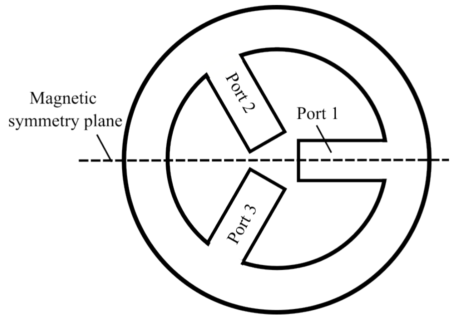

Figure 3. A front view of a tri-ridged waveguide used as an OMT, with port 1 associated with the central ridge which lies in the magnetic symmetry plane.

turn loss for a LHCP is given as

$$|S_{LL}|^2 = 1 - 3|\alpha_1 S_{M1} + S_{M2}(\alpha_2 + \alpha_3)|^2, \qquad (12)$$

where $S_{M1,2,3}$ is the transmission coefficient between the fundamental mode of the TRWG and excitation ports 1, 2 and 3 respectively, and α_n is a scaling term that has been calculated to synthesise the LHCP and is given as,

$$\begin{bmatrix} \alpha_1 \\ \alpha_2 \\ \alpha_3 \end{bmatrix} = \frac{\sqrt{2}}{3} \begin{bmatrix} 1 \\ 1\angle 120^\circ \\ 1\angle -120^\circ \end{bmatrix}. \qquad (13)$$

By enforcing the magnetic symmetry shown by [8], we have $S_{M2} = S_{M3}$. Substituting (13), we can rewrite (12) as

$$|S_{LL}|^2 = 1 - \frac{2}{3}|S_{M1} - S_{M2}|^2. \qquad (14)$$

Next, consider the S-parameters of the fundamental mode

$$S = \begin{bmatrix} S_{11} & S_{12} & S_{13} & S_{1M} \\ S_{21} & S_{22} & S_{23} & S_{2M} \\ S_{31} & S_{32} & S_{33} & S_{3M} \\ S_{M1} & S_{M2} & S_{M3} & S_{MM} \end{bmatrix}, \qquad (15)$$

with the subscripts indicating the coaxial excitation ports ($n \in 1,2,3$) and the fundamental mode (M). Taking the inner product of the fourth column gives

$$|S_{MM}|^2 = 1 - |S_{M1}|^2 - |S_{M2}|^2 - |S_{M3}|^2. \qquad (16)$$

Assuming again that $S_{M2} = S_{M3}$, due to magnetic symmetry, results in

$$|S_{MM}|^2 = 1 - |S_{M1}|^2 - 2|S_{M2}|^2. \qquad (17)$$

Returning now to the field distributions in a triangular waveguide described earlier, the coupling between the fundamental mode and the excitation ports of the OMT is a function of the electric field at the position of the excitation ports, which lie at ($\theta = 0^\circ, 120^\circ$ and 240°). These angles correspond to the boundary condition in (4) for $k = 0, 1, 2$, respectively, with the fundamental modes (S_{M1}, S_{M2}) corresponding to $k = 0$, 1 respectively. The ratio between S_{M1} and S_{M2} can be found from the electric field derived in (3) for a triangular waveguide ($s = 3$) with two cylindrical modes,

$$\frac{S_{M1}}{S_{M2}} = \frac{E_{\rho(k=0)}}{E_{\rho(k=1)}} = \frac{A_1 J_1(k_c\rho)\cos(0) + A_2 J_2(k_c\rho)\cos(0)]}{A_1 J_1(k_c\rho)\cos(\frac{2\pi}{3}) + A_2 J_2(k_c\rho)\cos(\frac{4\pi}{3})}, \tag{18}$$

simplifying to

$$\frac{S_{M1}}{S_{M2}} = -2. \tag{19}$$

This result is derived for an empty triangular waveguide but it still holds for the tri-ridged guides due to the three-fold symmetry. Substituting into (14) and (17) confirms the expected result that $S_{LL} = S_{MM}$ in single-mode triangular OMT structures. This result holds in full-wave simulations of these structures in CST.

5 Conclusion

This paper presented a method for analytically estimating the fields for the dominant TE and TM modes in RPWs using cylindrical mode expansions. The simplest two-mode analytical approximation results in RMS field errors of the order of 1% and maximum errors of a few percent. Higher-order cylindrical modes could be included by employing point-matching, as described in [15]. The analytical estimation was used show that the return loss for the CP wave was equal in magnitude to that of the fundamental mode in a tri-rdige OMT structure.

6 Acknowledgements

This research was supported by the South African Radio Astronomy Observatory, which is a facility of the National Research Foundation, an agency of the Department of Science and Innovation (Grant Number: 75322).

References

[1] P. E. Dewdney, P. J. Hall, R. T. Schilizzi, and T. J. L. W. Lazio, "The Square Kilometre Array," *Proc. IEEE*, vol. 97, no. 8, pp. 1482 – 1496, Aug. 2009.

[2] R. Selina, "The next-generation very large array: reference design overview," in *Proc. URSI AP-RASC*, New Delhi, India, Mar. 2019, pp. 1–1.

[3] A. H. Akgiray, "New technologies driving decade-bandwidth radio astronomy: quad-ridged flared horn and compound-semiconductor lnas," Ph.D. dissertation, California Institute of Technology, Pasadena, California, 2013.

[4] J. Flygare, "Dielectrically loaded quad-ridge flared horns for ultra wideband reflector feed applications in radio astronomy," Ph.D. dissertation, Chalmers University of Technology, Gothenburg, Sweden, 2022.

[5] R. Lehmensiek and D. I. L. de Villiers, "First order design of a quadruple-ridged flared horn for the ngvla band 1," in *Proc. 2022 16th Eur. Conf. Antennas and Propag. (EuCAP)*, Madrid, Spain, Mar. 2022, pp. 1–4.

[6] ——, "A method to design trapped-mode free quadruple-ridged flared horn antennas," in *Proc. 2023 17th Eur. Conf. Antennas and Propag. (EuCAP)*, Florence, Italy, Mar. 2023, pp. 1–4.

[7] M. A. Morgan, "Mutual coupling in compact orthomode transducers," Jan. 2011, accessed: Mar. 2024. [Online]. Available: https://arxiv.org/abs/1101.1929

[8] Z. du Toit, F. T. T. Mokhupuki, and D. I. L. de Villiers, "Tri-ridged waveguide orthomode transducer," in *Proc. 2023 Int. Microw. Antenna Symp (IMAS)*, Cairo, Egypt, Feb. 2023, pp. 240–242.

[9] A. Lötter and D. I. L. de Villiers, "Towards practical implementation of tri-ridged orthomode transducer," in *Proc. 2024 Int. Conf. Electromagn. in Adv. Appl. (ICEAA)*, Lisbon, Portugal, Sep. 2024, pp. 341–344.

[10] Q. Zheng, L. Ma, F. Xie, and J. Li, "Simple estimate for cut-off wave number of lowest-order TM mode of a hollow metallic waveguide of arbitrary cross-section," *Int. J. RF Microw. Comput.-Aided Eng*, vol. 10, pp. 159–163, May 2000.

[11] B. Ravelo and B. Mazari, "Characterization of the regular polygonal waveguide for rf em shielding application," *Prog. Electromagn. Res.*, vol. 12, pp. 95–105, Apr. 2010.

[12] D. M. Pozar, *Microwave engineering*, 4th ed. Hoboken, NJ: Wiley, 2012, ch. Transmission lines and waveguides, pp. 110–124.

[13] A. Lopez Moran, J. Córcoles, J. Ruiz-Cruz, J. Montejo-Garai, and J. Rebollar, "Electromagnetic scattering at the waveguide step between equilateral triangular waveguides," *ADV MATH PHYS*, vol. 2016, pp. 1–16, Jan. 2016.

[14] Dassault Systems, "CST studio suite 3D EM simulation and analysis software," 2023, accessed: Apr. 2024. [Online]. Available: https://www.3ds.com/products-services/simulia/products/cst-studio-suite/

[15] C. Y. Wang, "Cutoff frequencies of perturbed circular waveguides and polygonal waveguides," *J. Electromagn. Waves Appl.*, vol. 16:2, pp. 151–158, Apr. 2002.